Fruit Research

ARTICLE

Open Access

https://doi.org/10.48130/frures-0026-0002

Fruit Research **2026**, 6: e009

Genome-wide identification of histone acetyltransferases in banana and functional characterization of *MaHAG28* during fruit ripening

Qi Wang[1#], Yunke Zheng[2,3#], Muhammad Moaaz Ali[4], Jianbin Zhang[2,3], Hongxia Miao[2,3], Caihong Jia[2,3], Sijun Zheng[5,6], Xinguo Li[4*] and Juhua Liu[2,3*]

[1] *National Key Laboratory of Tropical Crop Breeding, School of Life and Health Sciences, Hainan University, Haikou 570228, China*
[2] *Institute of Tropical Bioscience and Biotechnology & Sanya Research Institute, Chinese Academy of Tropical Agricultural Sciences, Sanya 572024/Haikou 571101, China*
[3] *Hainan Key Laboratory for Protection and Utilization of Tropical Bioresources, Hainan Institute for Tropical Agricultural Resources, Chinese Academy of Tropical Agricultural Sciences, Haikou 571101, China*
[4] *School of Tropical Agriculture and Forestry, Hainan University, Haikou 570228, China*
[5] *Yunnan Key Laboratory of Green Prevention and Control of Agricultural Transboundary Pests, Agricultural Environment and Resources Institute, Yunnan Academy of Agricultural Sciences, Kunming 650205, China*
[6] *Bioversity International, Kunming 650205, China*
[#] Authors contributed equally: Qi Wang, Yunke Zheng
[*] Correspondence: 990895@hainanu.edu.cn (Li X); juhua69@126.com (Liu J)

Abstract

Protein acetylation and deacetylation are critical post-translational modifications (PTMs) that regulate diverse biological processes in eukaryotes. Although histone acetyltransferases (HATs) and histone deacetylases (HDACs) have been characterized in several plant species, a systematic analysis of HATs in banana (*Musa acuminata*) has been lacking. In this study, we identified 36 HAT genes (*MaHATs*) from the banana A genome and classified them into four families based on phylogenetic relationships and conserved domain architecture: 29 HAG, two HAM, four HAC, and one HAF members. Chromosomal distribution and synteny analyses revealed that genome duplication events have contributed to the expansion of the *MaHAT* family. Integrated transcriptomic and proteomic analyses across different fruit ripening stages indicated that several *MaHATs* exhibit ripening-associated expression patterns. Among them, *MaHAG28* was highly expressed in fruit and showed dynamic regulation at both transcript and protein levels during ripening. Functional analyses using transient overexpression and virus-induced gene silencing in banana fruit slices demonstrated that *MaHAG28* accelerates starch degradation and promotes fruit ripening. Collectively, this study provides the first comprehensive characterization of the HAT gene family in banana and identifies *MaHAG28* as a positive regulator of fruit ripening, thereby advancing our understanding of acetylation-mediated regulatory mechanisms in banana fruit development.

Citation: Wang Q, Zheng Y, Ali MM, Zhang J, Miao H, et al. 2026. Genome-wide identification of histone acetyltransferases in banana and functional characterization of *MaHAG28* during fruit ripening. *Fruit Research* 6: e009 https://doi.org/10.48130/frures-0026-0002

Introduction

Protein acetylation is a major and evolutionarily conserved post-translational modification (PTM) that occurs in both prokaryotes and eukaryotes[1–5]. This modification is generally classified into N-terminal acetylation and lysine acetylation[6]. N-terminal acetylation is typically irreversible, whereas lysine acetylation is dynamic and reversible, transferring an acetyl group from acetyl-CoA to the ε-amino group present on lysine residues. This reaction is catalyzed by lysine acetyltransferases (KATs), commonly referred to as histone acetyltransferases (HATs), and reversed by histone deacetylases (HDACs), thereby establishing a tightly regulated equilibrium that modulates protein stability, localization, and activity[7,8].

Protein acetylation was first identified on histones; consequently, enzymes responsible for catalyzing and removing acetyl groups were initially named histone acetyltransferases and histone deacetylases. However, accumulating evidence indicates that HATs target a broad range of non-histone substrates and participate in diverse biological processes beyond chromatin regulation[9]. Based on sequence homology and structural characteristics, plant and animal HATs/KATs are classified into four major families: the GNAT (Gcn5-related N-acetyltransferase) family, the MYST (MOZ-Ybf2/Sas3-Sas2-Tip60) family, the CBP (p300/CREB-binding protein) family, and the TAFII250 (TATA-binding protein-associated factor) family[7].

Among these, the GNAT family was the first to be identified and molecularly characterized[8]. Proteins belonging to this family share conserved structural features that enable the transfer of acetyl groups from acetyl-CoA to lysine residues, despite exhibiting substantial diversity in substrate specificity[9]. Collectively, these proteins constitute the GNAT superfamily, which is defined by four conserved sequence motifs (A–D), essential for acetyl-CoA binding and catalysis[10]. Based on domain organization, the GNAT superfamily can be further subdivided into four subfamilies: HPA2, GCN5, HAT1, and ELP3[11]. HPA2, initially identified as HAT1 in yeast, contains only the conserved acetyltransferase domain (Acetyltransf_1; Pfam00583)[12]. GCN5 proteins harbor an N-terminal HAT domain and a C-terminal bromodomain that functions as a chromatin-targeting module[13]. HAT1 proteins are characterized by an N-terminal, Hat1_N domain, and a C-terminal HAT domain, whereas ELP3 proteins contain both an ELP domain and a HAT domain. In contrast, members of the MYST, CBP/p300, and TAFII250 families lack the canonical GNAT-type HAT domain but retain acetyltransferase activity through distinct conserved domains, including MOZ_SAS, KAT11, and TBPb, respectively[11].

Bananas (*Musa* spp.) are among the top-produced food crops, serving as a primary source of food for millions of people[14]. The ripening of banana fruit is typically accompanied by starch degradation[15]. However, the research on acetylation modifications in bananas remains limited, with the existing body of work largely centered on HDACs, including their roles in fruit ripening mechanisms and stress resistance. However, studies linking acetylation to ripening quality traits, such as starch metabolism, are notably lacking. Histone deacetylase MaHDA1 has been identified to interact with the ethylene-responsive transcription factor MaERF11, thereby enhancing *MaERF11*-mediated repression of *MaACO1* transcription. This finding suggests that *MaERF11* recruits *MaHDA1* to its target genes to suppress ethylene biosynthesis through histone deacetylation[16]. Song et al.[17] identified a MYB transcription factor, *MaMYB4*, that interacts with *MaHDA2* in banana fruit. This interaction strengthens *MaMYB4*-mediated transcriptional repression of ω-3 fatty acid desaturase genes (*MaFADs*), thereby regulating fatty acid biosynthesis during fruit development. In addition, Luxmi et al.[18] reported that the combined application of an HDAC inhibitor and abscisic acid (ABA) differentially inhibited seed germination in wild-type and transgenic plants, indicating that *MaSIN3*-associated HDAC complexes participate in distinct aspects of ABA-mediated growth inhibition.

Despite these advances, the histone acetyltransferase gene families in banana have not yet been systematically identified or functionally characterized, and their potential roles in fruit ripening remain largely unknown. Given the central role of acetylation in transcriptional regulation and hormone signaling, a comprehensive analysis of banana HATs is essential for understanding epigenetic regulation of fruit development. This study conducted a genome-wide identification and classification of histone acetyltransferase genes (MaHATs) within the banana A genome. We further analyzed their phylogenetic relationships, conserved domains, gene structures, and expression patterns, with particular emphasis on candidates associated with fruit ripening. In addition, we functionally characterized *MaHAG28*, a GNAT family member, to elucidate its role in regulating banana fruit ripening. The results provide a foundational resource for future studies on HAT-mediated epigenetic regulation in banana and advance our understanding of acetylation-dependent mechanisms governing fruit ripening and plant development.

Materials and methods

Plant materials

Banana (*Musa* spp.) fruit of the cultivars 'Baxijiao' and 'Fenjiao' were obtained from the Banana Genetic Improvement Laboratory, Biotechnology Research Institute, Chinese Academy of Tropical Agricultural Sciences, Haikou. Fruit at the first maturity stage (I; approximately 80 d after flowering) were harvested and stored at 22 °C until they reached the second (II), and sixth (VI) maturity stages (according to the Banana Ripening Guide by the USDA's Agricultural Marketing Service) (Fig. 1). *Nicotiana benthamiana* plants (3–6 weeks old) were grown in a greenhouse at 25 °C under a 16 h light/8 h dark photoperiod and were used for transient expression assays.

Identification, sequence alignment, phylogenetic analysis, and protein structure prediction of the *MaHATs* gene family

Published amino acid sequences of histone acetyltransferases from *Arabidopsis thaliana*[19], *Oryza sativa*[20], and *Solanum lycopersicum*[11] were used as query sequences. BLAST searches were performed against the *Musa acuminata* A-genome (v2) using TBtools software. Candidate MaHAT proteins were identified based on sequence similarity and the presence of conserved acetyltransferase domains.

Multiple sequence alignments were performed, and phylogenetic trees were generated using MEGA11 with default parameters. Protein secondary structure was predicted using the Phyre2.2 online server in ALPHAFOLD/ALPHATHREAD mode (www.sbg.bio.ic.ac.uk/phyre2). Predicted secondary structures were visualized using ESPript (https://espript.ibcp.fr/ESPript/ESPript), and three-dimensional protein structures were displayed using EZMol (www.sbg.bio.ic.ac.uk/ezmol). Conserved domains of all identified MaHAT proteins were analyzed using the NCBI Conserved Domain Database (CDD; www.ncbi.nlm.nih.gov/cdd). The final identification of candidate MaHAT proteins was based on a dual stringent screening approach. Initially retrieved protein sequences must hit at least one known HAT-characteristic domain in the Conserved Domain Database (CDD). Simultaneously, these sequences must also be validated for the presence of the same HAT-characteristic domain in either the Pfam or SMART database. Only when two independent databases consistently confirm the presence of complete and functional HAT domains is a protein designated as a final candidate MaHAT.

Characterization of *MaHATs* genes and proteins

For each identified *MaHAT* gene, a 2,000 bp genomic sequence upstream of the translation start codon (ATG) was retrieved from the *M. acuminata* v2 genome using TBtools. Putative *cis*-acting regulatory elements within these promoter regions were predicted using the PlantCARE database (http://bioinformatics.psb.ugent.be/webtools/plantcare/html) and visualized with TBtools.

Physicochemical properties of the predicted *MaHAT* proteins, including molecular weight, isoelectric point (pI), hydrophobicity, hydrophilicity, and protein stability, were analyzed using the ExPASy ProtParam online tool (https://web.expasy.org/protparam).

Transcriptomic and proteomic data analysis

Total RNA was extracted from banana pulp samples using standard protocols. RNA quality and integrity were assessed prior to library construction. Poly(A)+ mRNA was isolated from high-quality total RNA, reverse-transcribed into cDNA, end-repaired, adenylated at the 3′ ends, and ligated to sequencing adapters. Following purification and PCR amplification, libraries were sequenced on an Illumina NovaSeq platform to generate 150-bp paired-end reads. The raw sequencing reads were further processed using the BMKCloud Eukaryotic Transcriptome Analysis Platform with a reference genome (BMK Cloud; www.biocloud.net), where high-quality reads were aligned to the reference genome for downstream analyses.

For proteomic analysis, total protein was extracted from banana pulp, and protein concentration was determined using the bicinchoninic acid (BCA) method. Proteins were digested with trypsin, and the resulting peptides were separated using a NanoElute ultra-high-performance liquid chromatography (UHPLC) system. Peptides were ionized using a CaptiveSpray ion source and analyzed on a timsTOF Pro mass spectrometer. MS/MS spectra were searched against a theoretical protein database derived from the reference genome. High-confidence peptide-spectrum matches were filtered based on scoring algorithms and mapped to their corresponding genes for quantitative analysis.

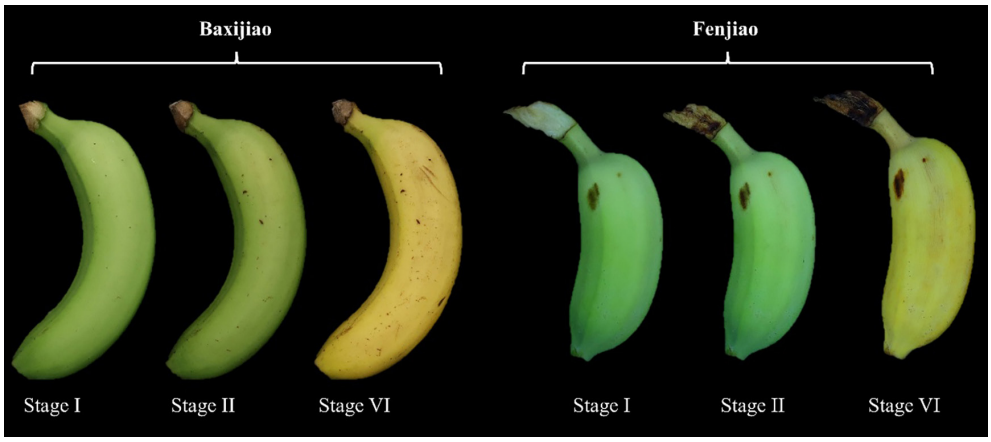

Fig. 1 Maturity stages of banana (*Musa* spp.) fruit used in this study. Fruit of the cultivars 'Baxijiao' and 'Fenjiao' were harvested at the first maturity stage (I; approximately 80 d after flowering) and subsequently stored at 22 °C until reaching the second (II), and sixth (VI) maturity stages, as defined by the USDA Agricultural Marketing Service Banana Ripening Guide.

Plasmid construction and subcellular localization in tobacco leaves

The full-length coding sequence of *MaHAG28* was cloned in-frame into the plant expression vector pCambia1300, generating a C-terminal GFP fusion under the control of the CaMV 35S promoter. Plasmid construction was performed using a homologous recombination-based cloning strategy. The resulting 35S:*MaHAG28*-GFP construct was introduced into *Agrobacterium tumefaciens* strain GV3101.

Transient expression assays were conducted by agroinfiltration of *N. benthamiana* leaves. GFP fluorescence was observed 2–3 d post-infiltration using a confocal laser scanning microscope. Nuclei were visualized by DAPI staining. Primers used for vector construction are listed in Supplementary Table S1.

Quantitative real-time PCR (qRT-PCR) analysis

Total RNA was extracted from banana pulp (cultivars 'Baxijiao' and 'Fenjiao') at maturity stages I, II, and VI using the RNAprep Pure Polysaccharide Polyphenol Plant Total RNA Extraction Kit (DP441; Tiangen, China). RNA quality was assessed, and first-strand cDNA was synthesized using the Maxima™ H Minus First Strand cDNA Synthesis Kit with dsDNase (K1682; Thermo Fisher Scientific).

The synthesized cDNA was diluted fivefold and used as a template for qRT-PCR. Reactions were performed using Hieff UNICON® Universal Blue qPCR SYBR Green Master Mix (11184ES08; Yeasen, China) on a QuantStudio™ 3 Real-Time PCR System (Thermo Fisher Scientific). Gene-specific primers are listed in Supplementary Table S1.

Transient overexpression and silencing in banana fruit slices

For transient overexpression assays, the full-length coding sequence of *MaHAG28* was cloned into the pCambia1300 vector. For virus-induced gene silencing (VIGS), a gene-specific fragment of *MaHAG28* was inserted into the pTRV2 vector. All constructs were generated using homologous recombination, and primers are listed in Supplementary Table S1. The recombinant plasmids were transformed into *Agrobacterium tumefaciens* strain GV3101.

Banana fruit slices were infiltrated with the corresponding *Agrobacterium* suspensions and co-cultured on Murashige and Skoog (MS) medium for 3–5 d. Starch accumulation was assessed by iodine-potassium iodide (I_2-KI) staining, and RNA was extracted from treated tissues to evaluate changes in *MaHAG28* transcript levels.

Measurement of physiological ripening parameters in banana fruit

Starch content in banana pulp was quantified using a spectrophotometric iodine-binding assay. Pulp tissue was homogenized, and soluble sugars were removed by repeated washing with anhydrous ethanol. Starch was subsequently extracted by boiling in 80% $Ca(NO_3)_2$ solution and reacted with a standardized 1% I_2-KI solution. Absorbance of the starch-iodine complex was measured at 620 nm, and starch concentration was calculated using a standard curve. Each experiment included three biological and three technical replicates.

Statistical analysis

Statistical analyses were performed using SPSS version 13[21]. One-way analysis of variance (ANOVA) was used to evaluate significant differences among treatments. Data are expressed as mean ± standard deviation (SD). Statistical significance is denoted as follows: as follows: * $p < 0.05$, ** $p < 0.01$, *** $p < 0.00$, and **** $p < 0.0001$. Graphical visualization was performed using GraphPad Prism version 10.

Results

Identification and phylogenetic analysis of *MaHATs*

To identify histone acetyltransferase genes in banana, reported HAT protein sequences from *Arabidopsis thaliana*, *Oryza sativa*, and *Solanum lycopersicum* were used as queries to search the *Musa acuminata* A-genome using TBtools. Candidate sequences with an E-value < 1×10^{-5} were retained for further analysis. After homology-based filtering and confirmation of conserved acetyltransferase domains, a total of 36 histone acetyltransferase genes (*MaHATs*) were conclusively identified in the banana A genome (Fig. 2; Supplementary Table S2).

The predicted MaHAT proteins exhibited substantial variation in size and molecular weight. Protein lengths ranged from 136 amino acids (aa) (MaHAM2) to 1,814 aa (MaHAF1), corresponding to molecular weights between 16.55 and 205.28 kDa (Supplementary Table S3). Based on conserved domain composition and sequence similarity, the identified MaHATs were classified into four canonical families: GNAT (MaHAG), MYST (MaHAM), CBP (MaHAC), and TAFII250 (MaHAF).

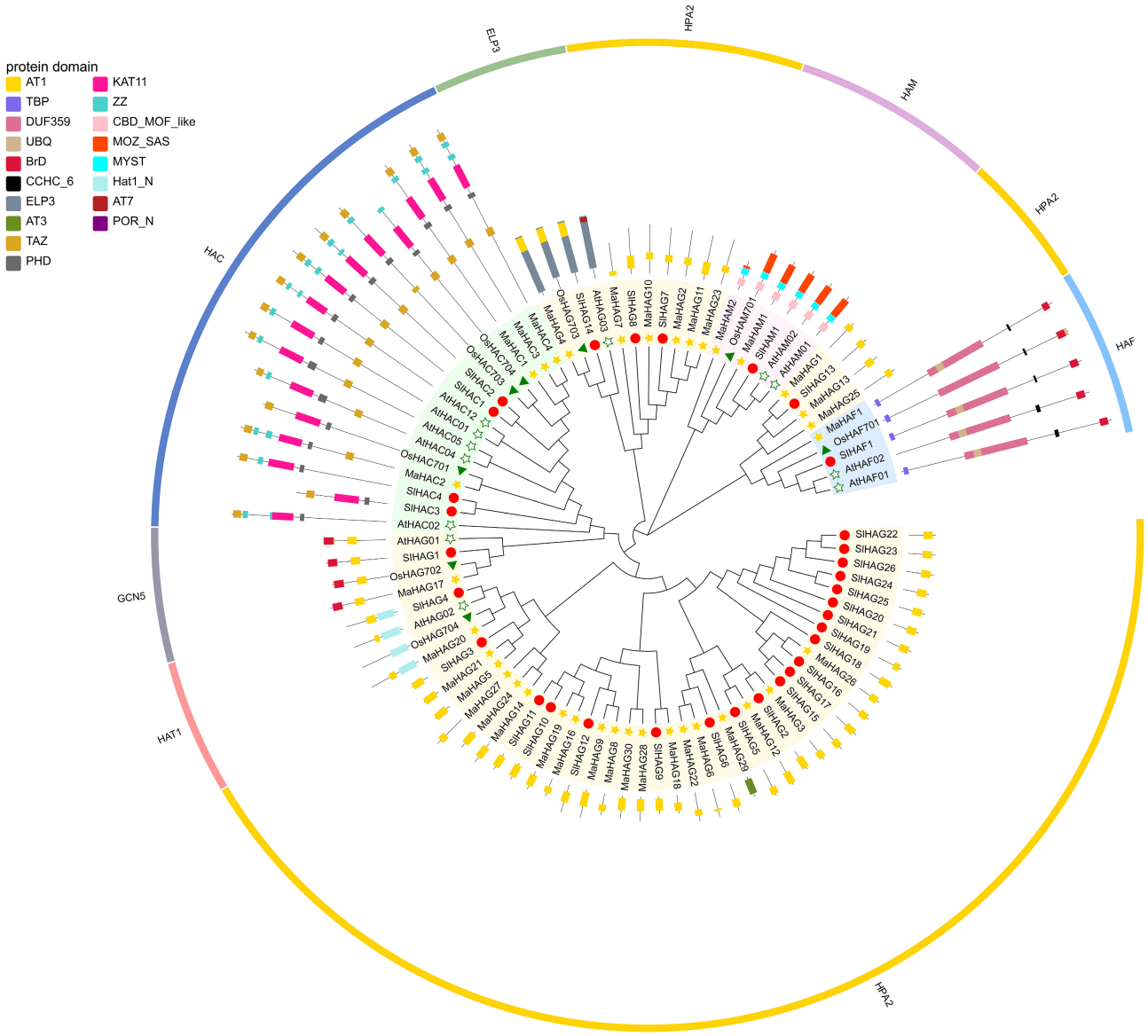

Fig. 2 Phylogenetic analysis of HATs proteins from the banana A genome, *A. thaliana*, *S. lycopersicum*, and *O. sativa*. The outermost ring indicates the family classification, and the middle ring annotates conserved domains identified within the amino acid sequences.

To elucidate the evolutionary relationships among *MaHATs*, a phylogenetic tree was generated based on the full-length amino acid sequences of banana HATs along with representative HATs from *A. thaliana*, *O. sativa*, and *S. lycopersicum*. The resulting phylogeny clearly separated *MaHATs* into distinct clades corresponding to the four established HAT families, thereby corroborating their family assignments and indicating strong evolutionary conservation of HAT classification across plant species (Fig. 2).

Chromosomal distribution and duplication analysis of *MaHATs*

To investigate the genomic distribution and evolutionary expansion of the *MaHAT* gene family, chromosomal localization and synteny analyses were performed. The 36 *MaHAT* genes were unevenly distributed across chromosomes 1–11 of the banana A genome (Fig. 3a). Chromosomes 4, 5, and 6 each harbored five *MaHAT* genes representing the highest gene densities among all chromosomes. All five *MaHAT* genes located on chromosome 4 belonged to the GNAT family. Chromosome 5 contained one CBP family member (*MaHAC1*) and four GNAT family members (*MaHAG11*, *MaHAG12*, *MaHAG13*, and *MaHAG30*). Chromosome 6 comprised one MYST family gene (*MaHAM1*), two CBP family genes (*MaHAC2* and *MaHAC3*), and two GNAT family genes (*MaHAG14* and *MaHAG16*). Chromosomes 3, 9, and 10 each contained four *MaHAT* genes, with all except *MaHAM2* (located on chromosome 10) belonging to the GNAT family. Chromosomes 7 and 11 harbored the fewest *MaHAT* genes, each containing a single gene (*MaHAC4* and *MaHAG26*, respectively). Notably, the sole TAFII250 family member, *MaHAF1* was located on chromosome 2.

Intraspecific synteny analysis identified six pairs of duplicated *MaHAT* genes, with each duplicated pair belonging to the same HAT family, suggesting that segmental duplications played a role in the expansion of this gene family in banana (Fig. 3b). To further explore the evolutionary conservation of *MaHATs*, interspecific synteny analyses were conducted between banana and three representative plant species: *A. thaliana*, *S. lycopersicum*, and *O. sativa*. Only two homologous gene pairs were detected between banana and *A.*

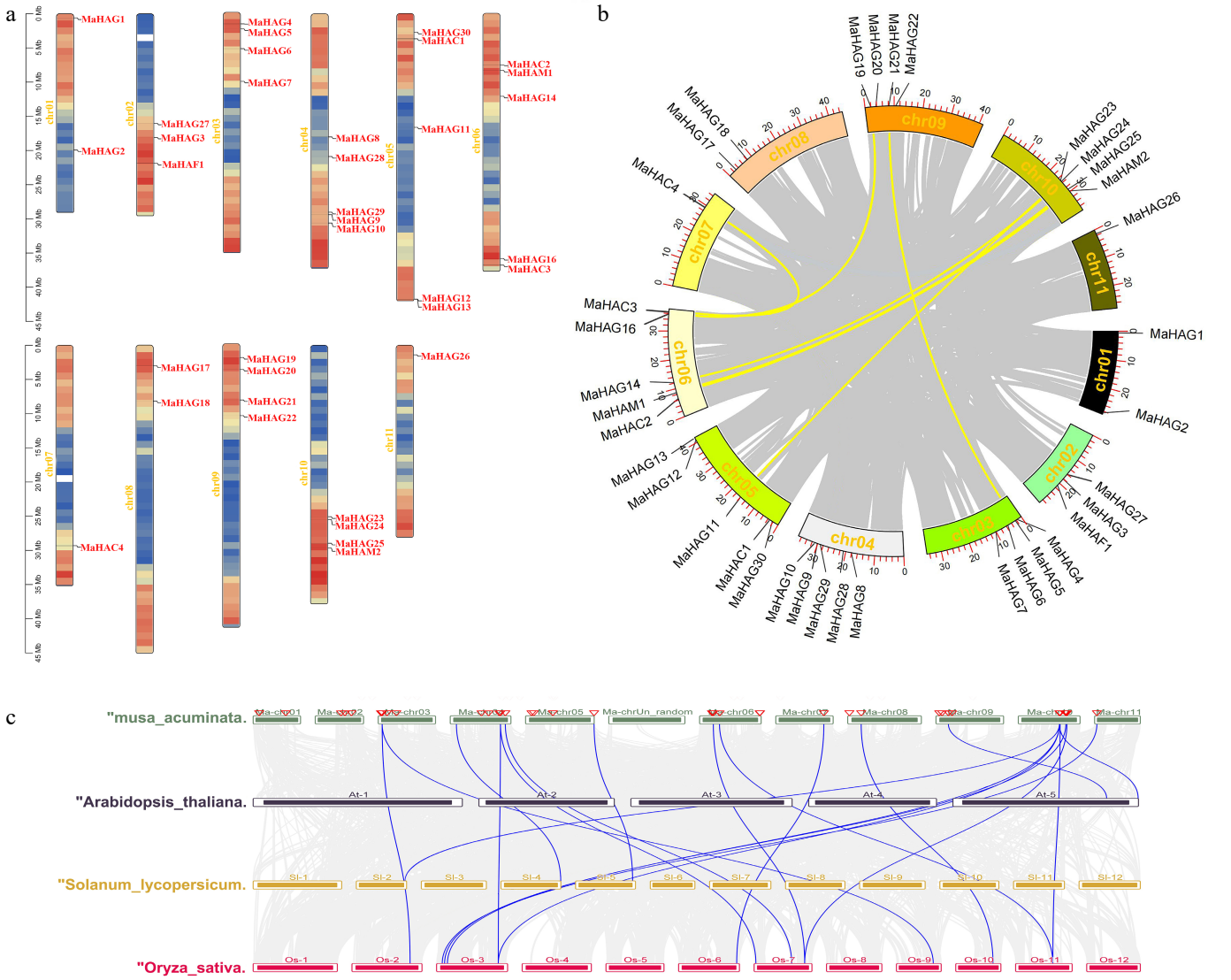

Fig. 3 (a) Chromosomal localization of identified *MaHATs* across the 11 banana chromosomes. (b) Intra-specific synteny analysis of the *MaHATs* loci. (c) Interspecific synteny analysis between *MaHATs* and *AtHATs*, *SlHATs*, and *OsHATs*.

thaliana, located on chromosomes 9 and 10 of the banana genome (Fig. 3c). In contrast, four homologous pairs were identified between banana and tomato, with two pairs located on chromosome 10 and the remaining pairs on chromosomes 4 and 5. Strikingly, 12 homologous gene pairs were detected between banana and rice, a monocot species, distributed across seven banana chromosomes (excluding chromosomes 1, 2, 5, and 9), with chromosome 10 containing the highest number of syntenic pairs (four). Among all *MaHATs*, *MaHAG23* exhibited conserved syntenic relationships with orthologs in all three comparative species, indicating a high degree of evolutionary conservation and suggesting a potentially fundamental role for this gene across diverse plant lineages.

Gene structure, conserved domains and *cis*-regulatory elements of *MaHAT* genes

Analysis of exon-intron organization revealed substantial structural diversity among *MaHAT* genes (Fig. 4a). *MaHAF1*, *MaHAC1*, *MaHAC3*, and *MaHAC4* exhibited long genomic sequences with complex exon-intron architectures. Notably, all four CBP family (*HAC*) members possessed extended coding sequences (CDSs), consistent with the large size and multidomain nature of CBP-type acetyltransferases. In contrast, genes belonging to the GNAT (*HAG*) and MYST (*HAM*) families generally displayed simpler gene structures. Several *HAG* genes, including *MaHAG3*, *MaHAG5*, *MaHAG7*, *MaHAG26*, *MaHAG28*, *MaHAG29*, and *MaHAG30*, contained a single CDS interrupted by very short introns, suggesting limited structural complexity.

Based on conserved domain composition, the 36 MaHAT proteins were classified into 29 GNAT (HAG), two MYST (HAM), four CBP (HAC), and one TAFII250 (HAF) family member (Fig. 2). Within the GNAT family, only one protein, MaHAG4, was assigned to the ELP3 subfamily, containing both an ELP3 domain and an upstream Acetyltransf_1 (AT1) domain. Consistent with observations in *A. thaliana*, *O. sativa*, and *S. lycopersicum*, each of which contains a single ELP3-type protein, MaHAG4 clustered closely with its orthologs in the phylogenetic tree, indicating strong evolutionary conservation.

Two additional GNAT subfamilies, GCN5 and HAT1, were each represented by a single gene in banana: MaHAG17 and MaHAG20, respectively. All GCN5-type proteins contained a conserved N-terminal AT1 domain and a C-terminal bromodomain (BrD), whereas

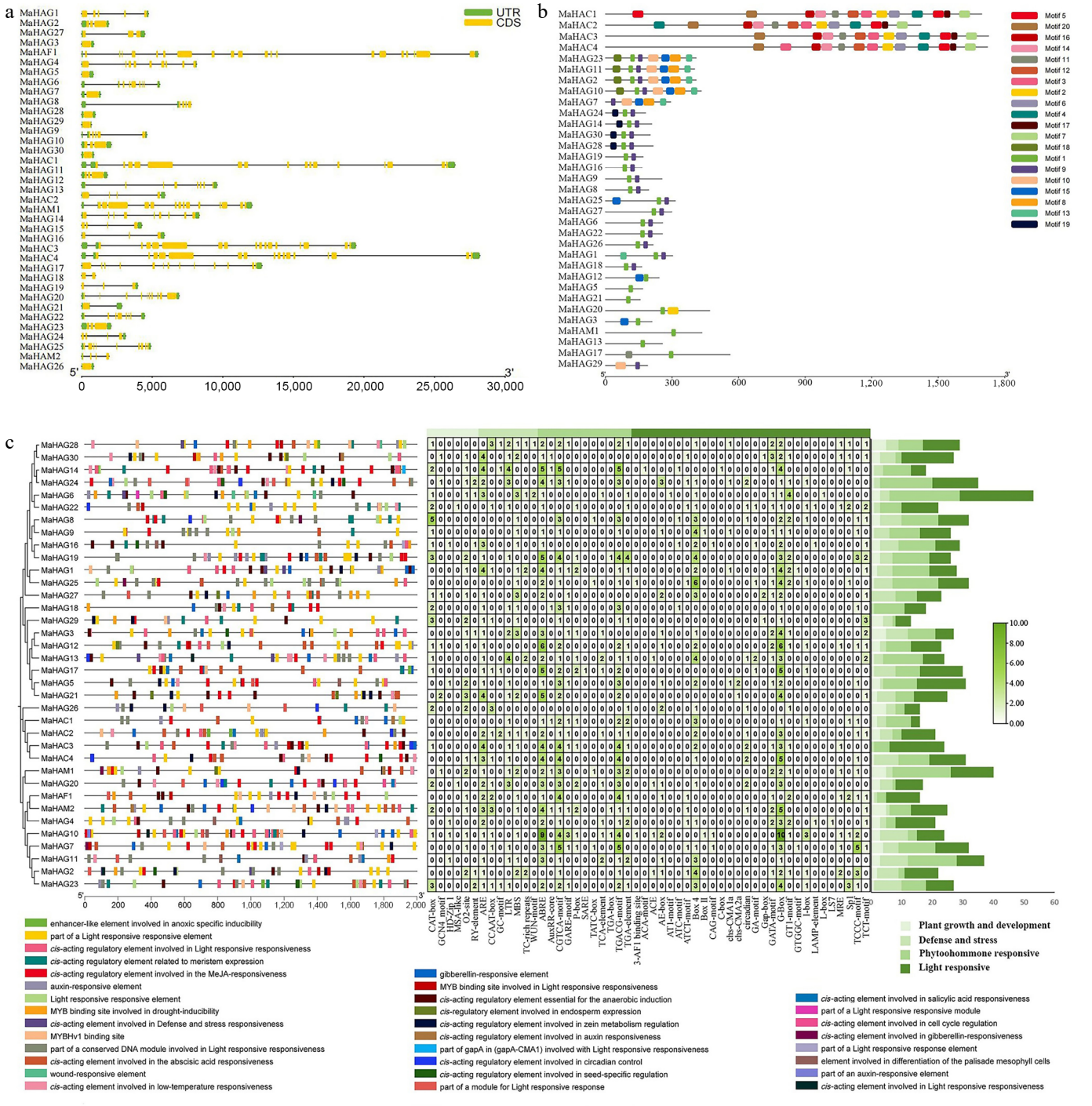

Fig. 4 (a) Analysis of *cis*-regulatory elements in the promoter regions of *MaHATs*. (b) Characterization of the coding sequence (CDS) architecture of *MaHATs*. (c) Analysis of conserved protein motifs in MaHATs sequences.

HAT1-type proteins harbored an N-terminal Hat1_N domain and a C-terminal AT1 domain. The remaining 26 GNAT proteins were classified as HPA2-type members. Phylogenetic analysis further divided these HPA2 proteins into three subgroups. One subgroup was dominated by tomato proteins and contained only three banana members (MaHAG6, MaHAG22, and MaHAG26), whereas the other two subgroups were predominantly composed of banana proteins. Within the largest subgroup, comprising 20 banana and seven tomato members, MaHAG27 formed a distinct branch, reflecting lower sequence similarity, and MaHAG29 also exhibited notable divergence. Domain analysis revealed that MaHAG29 contains an Acetyltransf_3 (AT3) domain spanning amino acids 21–155, distinguishing it from other HPA2 members.

Members of the HAC, HAM, and HAF families were relatively few in the banana A genome. The four HAC proteins (MaHAC1–MaHAC4) clustered with their orthologs from *A. thaliana*, *S. lycopersicum*, and *O. sativa*. Among them, MaHAC1, MaHAC3, and MaHAC4 displayed high mutual similarity, whereas MaHAC2 showed closer similarity to rice OsHAC701. All HAC proteins shared conserved KAT11 and PHD domains, with the PHD domain consistently located N-terminal to

KAT11. The number of TAZ and ZZ domains varied slightly among members, with up to two of each. TAZ domains were positioned at the termini of the domain architecture, while ZZ domains were located between the C-terminal TAZ and KAT11 domains. Only MaHAC1 contained a single ZZ domain, whereas MaHAC2–MaHAC4 each possessed two.

Two MYST family members, MaHAM1 and MaHAM2, were identified. MaHAM1 exhibited high similarity to HAM proteins from the other three plant species, whereas MaHAM2 encoded a much shorter protein due to truncation of the MOZ_SAS domain. In contrast, the CBD_MOF-like and MYST domains showed relatively minor variation between the two proteins. The single TAFII250 family member, *MaHAF1*, exhibited a conserved domain architecture consisting of an N-terminal TBP-binding domain, followed by DUF3591, UBQ, CCHC_6, and a C-terminal bromodomain. The UBQ domain was consistently located near the N-terminus of the DUF3591 domain, consistent with its orthologs.

Conserved motif analysis further supported family classification and phylogenetic relationships (Fig. 4b). Motif composition and arrangement were highly conserved within each HAT family. Notably, the three HPA2 subgroups within the GNAT family exhibited distinct motif patterns, consistent with their phylogenetic subdivision. Proteins belonging to unique classifications, such as MaHAG4 (ELP3 subfamily) and MaHAF1 (TAFII250 family) lacked the conserved motifs shared by other members, reflecting their divergent evolutionary origins.

To explore potential regulatory mechanisms, the 2 kb promoter regions upstream of the transcription start sites of MaHAT genes were analyzed for *cis*-acting regulatory elements (Fig. 4c). The majority of identified elements were associated with light responsiveness, followed by elements related to phytohormone signaling, abiotic stress responses, and growth and developmental regulation, suggesting that MaHATs may participate in diverse regulatory pathways.

Physicochemical properties and predicted subcellular localization of MaHAT proteins

To characterize the biochemical features of MaHAT proteins, their physicochemical properties were analyzed (Supplementary Table S3). The predicted isoelectric points (pI) of most MaHATs ranged from 5.0 to 9.0, indicating near-neutral charge properties, with the exception of MaHAG3, which exhibited a markedly high pI of 11.39. Based on the instability index, most MaHAT proteins were predicted to be unstable (index > 40), whereas only ten members were classified as stable. The aliphatic index, which reflects protein thermostability, ranged from 67.18 (MaHAG17) to 106.44 (MaHAG8), suggesting generally favorable thermal stability across the family. The grand average of hydropathicity (GRAVY) values were negative for most MaHATs, indicating a predominantly hydrophilic nature. However, MaHAG7, MaHAG8, MaHAG11, MaHAG23, and MaHAG26 exhibited positive GRAVY values, suggesting relatively hydrophobic properties. Subcellular localization predictions indicated that most MaHAT proteins are localized to the nucleus, cytoplasm, or chloroplast, consistent with their potential regulatory roles. Notably, MaHAG24 was predicted to localize to the peroxisome, suggesting possible functional diversification within the GNAT family.

Transcriptomic and proteomic profiling of *MaHATs* during banana fruit ripening and expression analysis of *MaHAG28*

To investigate the involvement of *MaHATs* in banana fruit ripening, transcriptomic and proteomic analyses were performed using fruit from two cultivars, 'Baxijiao' and 'Fenjiao', at three ripening stages (I, II, and VI). RNA-seq analysis revealed dynamic expression changes for several *MaHAT* genes during ripening (Fig. 5a). In both cultivars, transcript levels of *MaHAG27*, *MaHAG28*, *MaHAG30*, *MaHAM1*, *MaHAG17*, and *MaHAG20* decreased progressively during ripening. In contrast, *MaHAG19* showed increased expression, while *MaHAG14*, *MaHAG18*, and *MaHAG29* exhibited an initial increase followed by a decline. Overall, expression trends were largely conserved between the two cultivars. Notably, transcripts of the four *MaHAC* genes and *MaHAF1* were nearly undetectable throughout the ripening process in both cultivars, suggesting that CBP- and TAFII250-type acetyltransferases are not transcriptionally regulated during banana fruit ripening.

Proteomic analysis provided additional insight into MaHAT regulation at the protein level (Fig. 5a). In several cases, protein abundance did not directly correlate with transcript levels. For example, MaHAG28 protein abundance decreased during ripening in 'Baxijiao', consistent with its transcript profile, whereas in 'Fenjiao', protein levels initially increased before decreasing. Similarly, MaHAG26 protein levels mirrored transcript patterns in 'Fenjiao' but decreased in 'Baxijiao'. For *MaHAG4*, transcript levels initially decreased and then increased, whereas protein abundance decreased steadily in both cultivars. Interestingly, some genes with low transcript abundance in RNA-seq, such as *MaHAG21*, displayed detectable protein accumulation, indicating post-transcriptional regulation.

Based on transcriptomic data, we found that *MaHAG28* exhibited the highest expression level among all acetyltransferases in bananas at the initial ripening stage, with its expression gradually decreasing as ripening progressed. A consistent trend was also observed at the proteomic level. Thus, we propose that *MaHAG28* is likely a key gene triggering banana fruit ripening, warranting further investigation. The analysis of qRT-PCR confirmed this observation and provided more precise quantification (Fig. 5b). In 'Baxijiao', *MaHAG28* transcript levels peaked at stage II and decreased thereafter, whereas in 'Fenjiao', expression was highest at stage I and progressively decreased during ripening. Protein quantification revealed that MaHAG28 protein levels remained relatively stable between stages I and II in 'Baxijiao' but decreased significantly at stage VI. In contrast, despite decreasing transcript levels in 'Fenjiao', MaHAG28 protein abundance increased markedly at stage II relative to stage I. These findings imply post-transcriptional regulation of *MaHAG28* and suggest its potential role in controlling banana fruit ripening.

MaHAG28 displays dual subcellular localization and contributes to starch degradation in banana fruit

To further characterize MaHAG28 at the structural level, sequence alignment and three-dimensional protein modeling were performed. Multiple sequence alignment of MaHAG28 with yeast HPA2 demonstrated a high level of conservation within the GNAT-type histone acetyltransferase core domain, including several key residues previously reported to be involved in acetyl-CoA binding and catalysis in GNAT family proteins. Secondary structure annotation indicated conserved β-sheets and α-helices characteristic of GNAT/HAG family members. Consistent with this observation, homology-based structural modeling showed that MaHAG28 adopts a canonical GNAT fold, closely resembling the predicted structure of yeast HPA2 (Fig. 6a), supporting its classification as an HPA2-type GNAT protein.

To further elucidate the cellular context of *MaHAG28* in fruit ripening, its coding sequence was fused to GFP and transiently expressed in *Nicotiana benthamiana* leaves. Confocal microscopy revealed that the *MaHAG28*-GFP fusion protein was predominantly localized to

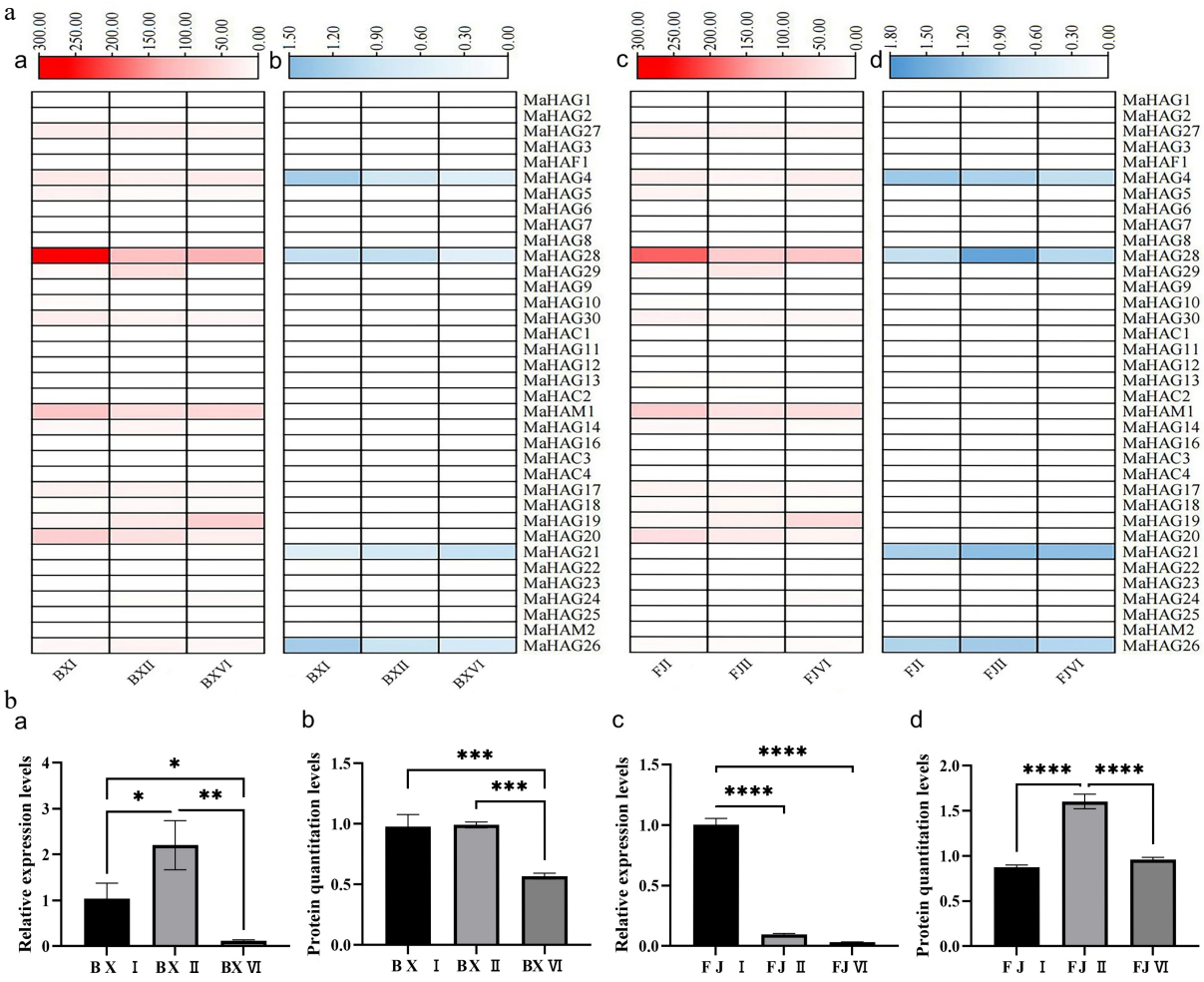

Fig. 5 (a) Integrated transcriptomic and proteomic data of MaHATs. Heatmaps (a) and (c) display the transcriptome profiles of the 'Baxijiao' and 'Fenjiao' varieties, respectively. Corresponding proteome profiles are presented in heatmaps (b) and (d) for the 'Baxijiao' and 'Fenjiao' varieties, respectively (both transcriptomic and proteomic analyses were performed with three biological replicates). (b) Expression and protein accumulation analysis of MaHAG28. Panels (a) and (c) show qRT-PCR analysis of *MaHAG28* transcript levels in 'Baxijiao' and 'Fenjiao' fruit at different ripening stages, respectively. The corresponding protein abundance levels are quantified in panels (b) and (d).

the nucleus, which is consistent with a potential involvement in nuclear regulatory processes (Fig. 6b). In addition, GFP fluorescence was also detected in the cytoplasm, indicating dual subcellular localization and suggesting that MaHAG28 may participate in both nuclear and cytoplasmic regulatory pathways. However, the precise molecular targets and biochemical activity of MaHAG28 remain to be determined.

As starch degradation is a hallmark of banana fruit ripening, starch content was measured in banana fruit slices following transient overexpression or virus-induced gene silencing (VIGS) of *MaHAG28* (Fig. 6c, d). Overexpression of *MaHAG28* resulted in a significant reduction in starch content compared with control samples. Although silencing of *MaHAG28* did not lead to a statistically significant increase in starch content, a clear upward trend was observed (Fig. 6e). Collectively, these results support the conclusion that *MaHAG28* contributes to the starch degradation and banana fruit ripening as a positive regulator.

Discussion

Protein acetylation is a fundamental post-translational modification that regulates protein stability, localization, and activity. The dynamic balance between acetylation and deacetylation, mediated by acetyltransferases and deacetylases, underpins numerous biological processes. In plants, accumulating evidence links acetylation to fruit metabolism and quality formation[22,23], as well as to the regulation of fruit ripening[16,24]. Although plant acetyltransferases have been extensively investigated[25,26], most studies have focused on vegetative growth and development, including the regulation of photosynthesis[27,28], seed fatty acid biosynthesis[29], jasmonate-responsive transcription[30], chlorophyll biosynthesis and chloroplast development[31], and ethylene signaling pathways[32]. In contrast, the direct involvement of acetyltransferases in fruit ripening remains poorly understood.

Fruit ripening is a complex developmental transition accompanied by extensive transcriptional reprogramming and metabolic remodeling; processes that are increasingly recognized to involve epigenetic regulation. There is a consensus among earlier studies regarding the crucial importance of histone deacetylation in ripening control. For example, *MdHDA19* suppresses apple fruit ripening by reducing histone acetylation levels[33], while in tomato, *SlHDA1* and *SlHDA3* form a repressive complex that inhibits the expression of ripening-associated genes through promoter deacetylation[34]. These findings collectively suggest a negative regulatory role for

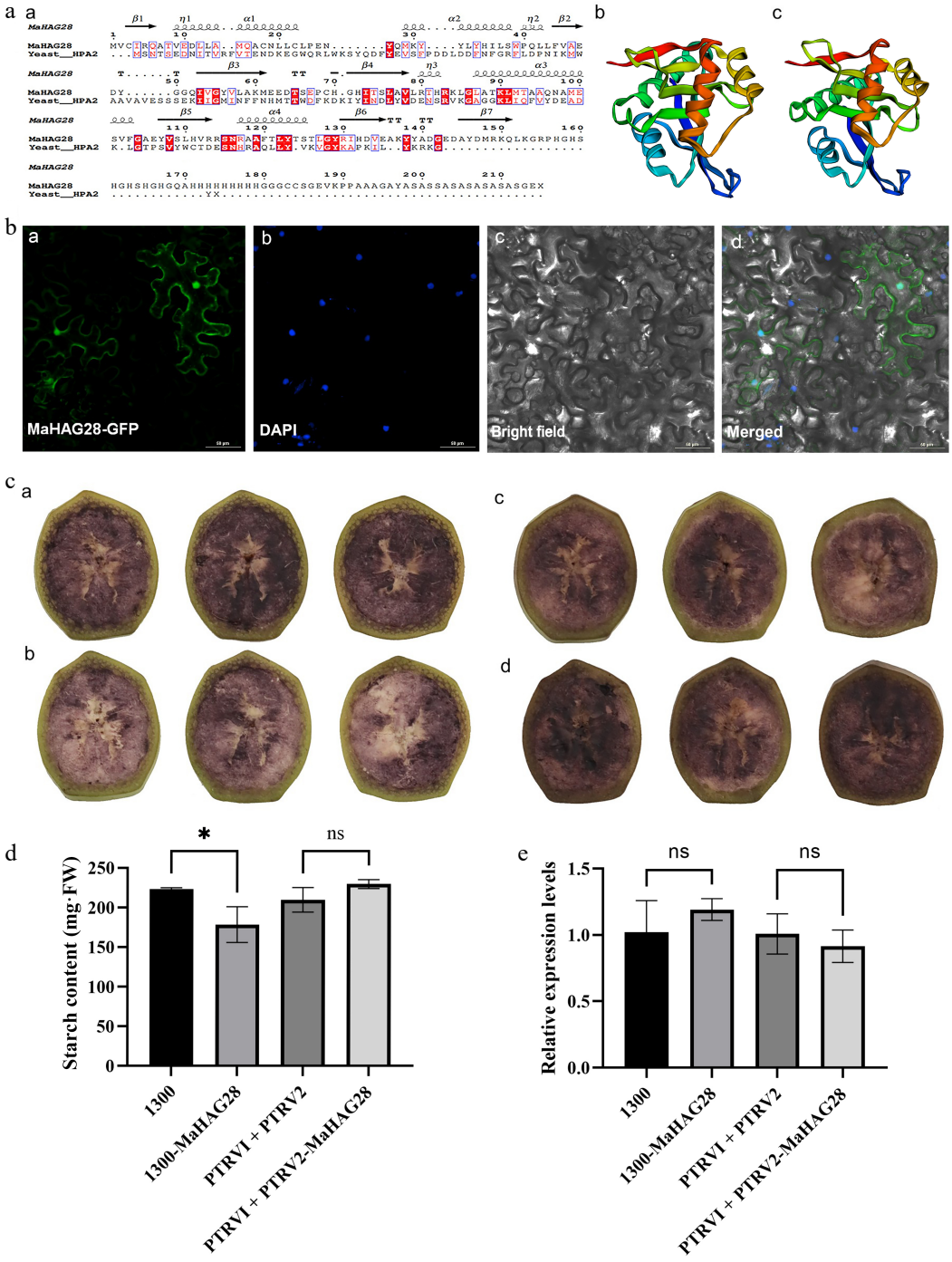

Fig. 6 (a) Comparison of MaHAG28 and yeast HPA2 secondary structures (a), and predicted three-dimensional structure of (b) MaHAG28, and (c) yeast HPA2. (b) Subcellular localization of MaHAG28 in tobacco leaf epidermal cells. GFP signal is detected in both the nucleus and cytoplasm (a). DAPI staining was used as a nuclear marker, (b). Scale bar = 50 μm. (c) Iodine-potassium iodide (0.5% I_2-KI) staining of banana fruit slices following transient overexpression or VIGS-mediated silencing of MaHAG28 (30 s incubation). Control groups transformed with empty vectors (a) pCambia1300, and (c) PTRV1 + PTRV2, respectively. Experimental groups transformed with (b) pCambia1300-*MaHAG28*, and (c) PTRV1 + PTRV2-*MaHAG28*, respectively. (d) Starch content in fruit slices across experimental groups. (e) Relative expression levels of *MaHAG28* in fruit slices across experimental groups.

deacetylation during ripening and imply that acetylation may act as a positive driver of this process. However, direct functional evidence supporting a promotive role of acetyltransferases in fruit ripening has been limited. To address this gap, we systematically identified HATs in the banana A genome and examined their potential involvement in ripening across different developmental stages.

In this study, we identified 36 *MaHATs* in the banana A genome, representing one of the largest HAT gene families reported in plants to date[24,35–38]. This expansion is likely attributable to the complex evolutionary history of the banana, which has undergone multiple whole-genome duplication events[39]. Consistent with this, chromosomal distribution and synteny analyses revealed both intra- and interspecific duplication patterns, supporting a major contribution of genome duplication to *MaHAT* family expansion. Notably, *MaHAG23* emerged as the most evolutionarily conserved HAT among the species examined, underscoring its likely fundamental

role in plant biology. Interestingly, *MaHAG23* has a paralog, *MaHAG11*, on chromosome 5 that lacks clear syntenic counterparts in other species. This observation suggests that *MaHAG11* may have arisen from a banana-specific duplication event followed by functional divergence. The reduced expression of *MaHAG23* during fruit ripening further implies a potential inhibitory role in this process, highlighting functional diversification among HAT family members.

To further elucidate the role of acetyltransferases in banana fruit ripening, we integrated transcriptomic, proteomic, and functional analyses. It is well established that transcript abundance does not necessarily correlate with protein levels or activity[40], emphasizing the importance of protein-level investigation. Among the identified HATs, *MaHAG28* showed a strong association with ripening-related processes. Transient overexpression of *MaHAG28* in banana fruit slices resulted in a significant reduction in starch content, indicating an acceleration of starch degradation, a hallmark of banana ripening. In contrast, transient silencing of *MaHAG28* via virus-induced gene silencing did not produce a statistically significant change in starch content. When considered alongside proteomic data revealing substantial pre-existing accumulation of *MaHAG28* protein, these results suggest that short-term suppression at the transcript level may be insufficient to counteract its functional effects[41]. This observation underscores the stability and potential longevity of acetyltransferase proteins during ripening.

Structural and cellular analyses further support a direct regulatory role of MaHAG28 in protein acetylation. Domain analysis classified MaHAG28 as an HPA2-type acetyltransferase belonging to the GNAT superfamily, whose members share a highly conserved catalytic fold despite low primary sequence similarity[12]. Yeast HPA2 has been shown to acetylate histones H3 and H4, with a preference for H3K14, and its tetrameric structure facilitates diverse modifications on histone tails. Consistent with this, homology modeling revealed that MaHAG28 adopts a GNAT-like fold closely resembling that of yeast HPA2, despite limited sequence conservation (Fig. 5a). Moreover, subcellular localization analysis demonstrated that MaHAG28 is localized to the nucleus, supporting its potential role in chromatin modification. The functional analysis of MaHAG28 suggests that histone acetyltransferases may act as positive regulators of fruit ripening, indicating a positive association between acetylation-related processes and ripening progression, an idea that is further supported by observations in grape fruit[23]. Together, these findings support the classification of MaHAG28 as an HPA2-type GNAT family protein with conserved structural features and nuclear localization, consistent with a potential regulatory role in acetylation-associated processes during fruit ripening. Nonetheless, the precise molecular substrates and catalytic activity of MaHAG28 remain to be elucidated.

Based on amino acid sequence alignment as well as phylogenetic and structural analyses, MaHAG28 shows similarity to NAA10/HPA2-type acetyltransferases. NAA10 was originally characterized as an N-terminal acetyltransferase lacking lysine acetyltransferase activity[42]; however, subsequent *in vitro* studies have demonstrated that, under specific conditions, NAA10 can also exhibit lysine acetyltransferase activity[43,44], suggesting functional flexibility within this protein class. In this context, the dual subcellular localization of MaHAG28 in both the cytoplasm and nucleus raises the possibility that it may participate in multiple acetylation-related processes, potentially including N-terminal acetylation of cytoplasmic proteins and lysine acetylation of nuclear proteins. Nevertheless, in the absence of direct biochemical evidence, any inference regarding NAT or KAT activity of MaHAG28 remains speculative. Future studies employing enzymatic assays and substrate identification will be required to define its catalytic specificity and direct molecular targets.

In summary, this study comprehensively characterizes the HAT gene family across the banana genome, identifying 36 *MaHATs* within the A genome. Functional analysis of the HAG family member *MaHAG28* demonstrates that its overexpression accelerates starch degradation and promotes fruit ripening. These findings reveal a previously under-appreciated role for acetyltransferases in banana fruit ripening and establish a direct link between acetylation and ripening-associated metabolic reprogramming. More broadly, our results highlight the functional diversity of plant acetyltransferases and provide a foundation for future studies aimed at manipulating epigenetic regulators to improve fruit quality and postharvest performance.

Conclusions

In this study, we performed a comprehensive genome-wide identification and characterization of histone acetyltransferases in banana (*Musa acuminata*, A genome), revealing a total of 36 *MaHAT* genes. Phylogenetic, structural, chromosomal distribution, and synteny analyses indicated that the *MaHAT* family has undergone substantial expansion, likely driven by whole-genome duplication events, and has experienced functional diversification during banana evolution. Expression profiling further suggested that several *MaHATs* are associated with fruit ripening, highlighting a potential role for acetylation in regulating this complex developmental process. Functional investigation of the HAG family member *MaHAG28* demonstrated that it acts as a positive regulator of banana fruit ripening. Transient overexpression of *MaHAG28* significantly promoted starch degradation, while subcellular localization and structural analyses supported its role as a functional acetyltransferase with conserved GNAT-like architecture. The similarity of MaHAG28 to HPA2/NAA10-type acetyltransferases and its dual localization suggest that it may integrate N-terminal and lysine acetylation to fine-tune protein function during ripening. Overall, our findings provide direct evidence that histone acetyltransferases contribute to the epigenetic regulation of banana fruit ripening. This work not only expands the current understanding of acetylation-mediated control of fruit development, but also establishes a valuable genomic and functional resource for future studies targeting acetyltransferases involved in banana growth, stress responses, and fruit quality improvement.

Ethical statements

Not applicable.

Author contributions

The authors confirm their contributions to the paper as follows: study conception and design: Wang Q, Zheng Y, Li X, Liu J; literature review: Wang Q; draft manuscript preparation: Wang Q, Ali MM, Miao H, Jia C, Zheng S; critical revision: Zheng Y, Zhang J, Li X, Liu J. All authors reviewed the results and approved the final version of the manuscript.

Data availability

The RNA-seq raw reads have been deposited in the NCBI Sequence Read Archive (SRA) under the accession number PRJNA343716. The proteomics raw data is not publicly available at this time but can be obtained from the corresponding author upon reasonable request via email.

Acknowledgments

The authors express their gratitude to the funding agencies and projects that supported this work, including the project of the National Key Laboratory for Tropical Crop Breeding (SKLTCBQN202511), the Hainan Province Science and Technology Special Fund (ZDYF2023XDNY179), Hainan Province Youth Fund (324QN319), and the earmarked fund for China Agriculture Research System (CARS-31).

Conflict of interest

The authors declare that they have no conflict of interest.

Supplementary information accompanies this paper online at: https://doi.org/10.48130/frures-0026-0002.

Dates

Received 31 December 2025; Revised 4 February 2026; Accepted 10 February 2026; Published online 10 March 2026

References

[1] Kouzarides T. 2000. Acetylation: a regulatory modification to rival phosphorylation? *The EMBO Journal* 19:1176–1179

[2] Lusser A, Kölle D, Loidl P. 2001. Histone acetylation: lessons from the plant kingdom. *Trends in Plant Science* 6:59–65

[3] Narita T, Weinert BT, Choudhary C. 2019. Functions and mechanisms of non-histone protein acetylation. *Nature Reviews Molecular Cell Biology* 20:156–174

[4] Zhang J, Sprung R, Pei J, Tan X, Kim S, et al. 2009. Lysine acetylation is a highly abundant and evolutionarily conserved modification in *Escherichia coli*. *Molecular & Cellular Proteomics* 8:215–225

[5] Allfrey VG, Faulkner R, Mirsky AE. 1964. Acetylation and methylation of histones and their possible role in the regulation of RNA synthesis. *Proceedings of the National Academy of Sciences of the United States of America* 51:786–794

[6] Hollebeke J, Van Damme P, Gevaert K. 2012. N-terminal acetylation and other functions of N^{α}-acetyltransferases. *Biological Chemistry* 393:291–298

[7] Kumar V, Thakur JK, Prasad M. 2021. Histone acetylation dynamics regulating plant development and stress responses. *Cellular and Molecular Life Sciences* 78:4467–4486

[8] Kleff S, Andrulis ED, Anderson CW, Sternglanz R. 1995. Identification of a gene encoding a yeast histone H4 acetyltransferase. *Journal of Biological Chemistry* 270:24674–24677

[9] Sternglanz R, Schindelin H. 1999. Structure and mechanism of action of the histone acetyltransferase Gcn5 and similarity to other *N*-acetyltransferases. *Proceedings of the National Academy of Sciences of the United States of America* 96:8807–8808

[10] Neuwald AF, Landsman D. 1997. GCN5-related histone *N*-acetyltransferases belong to a diverse superfamily that includes the yeast SPT10 protein. *Trends in Biochemical Sciences* 22:154–155

[11] Aiese Cigliano R, Sanseverino W, Cremona G, Ercolano MR, Conicella C, et al. 2013. Genome-wide analysis of histone modifiers in tomato: gaining an insight into their developmental roles. *BMC Genomics* 14:57

[12] Angus-Hill ML, Dutnall RN, Tafrov ST, Sternglanz R, Ramakrishnan V. 1999. Crystal structure of the histone acetyltransferase Hpa2: a tetrameric member of the Gcn5-related *N*-acetyltransferase superfamily. *Journal of Molecular Biology* 294:1311–1325

[13] Dhalluin C, Carlson JE, Zeng L, He C, Aggarwal AK, et al. 1999. Structure and ligand of a histone acetyltransferase bromodomain. *Nature* 399:491–496

[14] Miao H, Zhang J, Zheng Y, Jia C, Hu Y, et al. 2025. Shaping the future of bananas: advancing genetic trait regulation and breeding in the postgenomics era. *Horticulture Research* 12:uhaf044

[15] Zhu Z, Sun P, Jin Y, Jin Z, Sun J, et al. 2026. Revealing the role of the *MaLSF1* gene in fruit starch degradation and its regulatory transcription factors in *Musa acuminata*. *Postharvest Biology and Technology* 231:113902

[16] Han YC, Kuang JF, Chen JY, Liu XC, Xiao YY, et al. 2016. Banana transcription factor MaERF11 recruits histone deacetylase MaHDA1 and represses the expression of *MaACO1* and *Expansins* during fruit ripening. *Plant Physiology* 171:1070–1084

[17] Song C, Yang Y, Yang T, Ba L, Zhang H, et al. 2019. MaMYB4 recruits histone deacetylase MaHDA2 and modulates the expression of ω-3 fatty acid desaturase genes during cold stress response in banana fruit. *Plant & Cell Physiology* 60:2410–2422

[18] Luxmi R, Garg R, Srivastava S, Sane AP. 2017. Expression of the SIN3 homologue from banana, *MaSIN3*, suppresses ABA responses globally during plant growth in Arabidopsis. *Plant Science* 264:69–82

[19] Pandey R, Müller A, Napoli CA, Selinger DA, Pikaard CS, et al. 2002. Analysis of histone acetyltransferase and histone deacetylase families of *Arabidopsis thaliana* suggests functional diversification of chromatin modification among multicellular eukaryotes. *Nucleic Acids Research* 30:5036–5055

[20] Liu X, Luo M, Zhang W, Zhao J, Zhang J, et al. 2012. Histone acetyltransferases in rice (*Oryza sativa* L.): phylogenetic analysis, subcellular localization and expression. *BMC Plant Biology* 12:145

[21] IBM Corp. 2022. *IBM SPSS Statistics for Windows*. Armonk, NY: IBM Corp. www.ibm.com/products/spss

[22] Yin XR, Xie XL, Xia XJ, Yu JQ, Ferguson IB, et al. 2016. Involvement of an ethylene response factor in chlorophyll degradation during citrus fruit degreening. *The Plant Journal* 86:403–412

[23] Jia H, Zuo Q, Sadeghnezhad E, Zheng T, Chen X, et al. 2023. HDAC19 recruits ERF4 to the *MYB5a* promoter and diminishes anthocyanin accumulation during grape ripening. *The Plant Journal* 113:127–144

[24] Cai Y, Xu M, Liu J, Zeng H, Song J, et al. 2022. Genome-wide analysis of histone acetyltransferase and histone deacetylase families and their expression in fruit development and ripening stage of pepper (*Capsicum annuum*). *Frontiers in Plant Science* 13:971230

[25] Xu X, He XJ. 2025. Plant histone acetyltransferase complexes: conserved and plant-specific characteristics. *Current Opinion in Plant Biology* 88:102815

[26] Liu X, Yang S, Yu CW, Chen CY, Wu K. 2016. Histone acetylation and plant development. *Methods in Enzymology* 40:173–199

[27] Boycheva I, Bonchev G, Manova V, Stoilov L, Vassileva V. 2024. How histone acetyltransferases shape plant photomorphogenesis and UV response. *International Journal of Molecular Sciences* 25:7851

[28] Cai L, Li B, Zhou Q, Du J, Yang W, et al. 2025. N-acetyltransferase 10 catalyzes RNA N^4-acetylcytidine to regulate photosynthesis in rice. *Cell Reports* 44:115428

[29] Wang T, Xing J, Liu X, Liu Z, Yao Y, et al. 2016. Histone acetyltransferase general control non-repressed protein 5 (GCN5) affects the fatty acid composition of *Arabidopsis thaliana* seeds by acetylating *fatty acid desaturase 3 (FAD3)*. *The Plant Journal* 88:794–808

[30] An C, Deng L, Zhai H, You Y, Wu F, et al. 2022. Regulation of jasmonate signaling by reversible acetylation of TOPLESS in *Arabidopsis*. *Molecular Plant* 15:1329–1346

[31] Peng Y, Peng T, Chu Y, Yan W, Yao R, et al. 2025. *Arabidopsis* HOOKLESS1 acts as a histone acetyltransferase to promote cotyledon greening during seedling de-etiolation. *Proceedings of the National Academy of Sciences of the United States of America* 122:e2425647122

[32] Li C, Xu J, Li J, Li Q, Yang H. 2014. Involvement of *Arabidopsis* histone acetyltransferase *HAC* family genes in the ethylene signaling pathway. *Plant and Cell Physiology* 55:426–435

[33] Hu Y, Han Z, Wang T, Li H, Li Q, et al. 2022. Ethylene response factor MdERF4 and histone deacetylase MdHDA19 suppress apple fruit ripening through histone deacetylation of ripening-related genes. *Plant Physiology* 188:2166–2181

[34] Deng H, Chen Y, Liu Z, Liu Z, Shu P, et al. 2022. SlERF. F12 modulates the transition to ripening in tomato fruit by recruiting the co-repressor TOPLESS and histone deacetylases to repress key ripening genes. *The Plant Cell* 34:1250−1272

[35] Li H, Chen Y, Dai Y, Yang L, Zhang S. 2024. Genome-wide identification and expression analysis of histone deacetylase and histone acetyltransferase genes in response to drought in poplars. *BMC Genomics* 25:657

[36] Skarzyńska-Łyżwa A, Turek S, Pisz M, Aparna A, Pląder W, et al. 2025. Genome-wide identification and characterization of histone acetyltransferases and deacetylases in cucumber, and their implication in developmental processes. *Genes* 16:127

[37] Gao S, Li L, Han X, Liu T, Jin P, et al. 2021. Genome-wide identification of the histone acetyltransferase gene family in *Triticum aestivum*. *BMC Genomics* 22:49

[38] Jin P, Gao S, He L, Xu M, Zhang T, et al. 2021. Genome-wide identification and expression analysis of the histone deacetylase gene family in wheat (*Triticum aestivum* L.). *Plants* 10:19

[39] Li X, Yu S, Cheng Z, Chang X, Yun Y, et al. 2024. Origin and evolution of the triploid cultivated banana genome. *Nature Genetics* 56:136−142

[40] Liu Y, Beyer A, Aebersold R. 2016. On the dependency of cellular protein levels on mRNA abundance. *Cell* 165:535−550

[41] Wei W, Yang YY, Chen JY, Lakshmanan P, Kuang JF, et al. 2023. MaNAC029 modulates ethylene biosynthesis and fruit quality and undergoes MaXB3-mediated proteasomal degradation during banana ripening. *Journal of Advanced Research* 53:33−47

[42] Magin RS, March ZM, Marmorstein R. 2016. The N-terminal acetyltransferase Naa10/ARD1 does not acetylate lysine residues. *Journal of Biological Chemistry* 291:5270−5277

[43] Vo TTL, Jeong CH, Lee S, Kim KW, Ha E, et al. 2018. Versatility of ARD1/NAA10-mediated protein lysine acetylation. *Experimental & Molecular Medicine* 50:1−13

[44] Vo TTL, Park JH, Lee EJ, Nguyen YTK, Han BW, et al. 2020. Characterization of lysine acetyltransferase activity of recombinant human ARD1/NAA10. *Molecules* 25:588